Growth and Characterization of $MnBi_2Te_4$ Magnetic Topological Insulator

A. Saxena[1,2,a)], P. Rani[1], V. Nagpal[3], S. Patnaik[3] and V.P.S. Awana[1,2]

[1]*CSIR-National Physical Laboratory, K.S. Krishnan Marg, New Delhi-110012, India.*
[2]*Academy council of scientific and industrial Research, Ghaziabad U.P.-201002, India*
[3]*School of Physical Sciences, Jawaharlal Nehru University, New Delhi-110067,India*

[a)]Corresponding Author: kingofrmu@gmail.com

Abstract. We report successful growth of magnetic topological insulator (MTI) $MnBi_2Te_4$singlecrystalby solid state reaction route via self flux method. The phase formation of $MnBi_2Te_4$singlecrystalis strongly dependent on the heat treatment.$MnBi_2Te_4$is grown in various phases i.e., $MnBi_4Te_7$, $MnBi_6Te_{10}$ and MnTe as seen in powder X-ray diffraction (PXRD) of crushed resultant crystal. The Rietveld analysis shows some impurity lines along with the main phase $MnBi_2Te_4$. Low temperature (10K) magneto-resistance (MR) in applied magnetic field of up to 6 Tesla exhibited –ve MR below 0.5 Tesla and +ve for higher fields. The studied $MnBi_2Te_4$, MTI crystal could be a possible candidate for Quantum Anomalous Hall (QAH) effect. Here we are reporting a newly discovered magnetic topological insulator $MnBi_2Te_4$having non-trivial symmetry as well as strong Spin-Orbit Coupling forQAH effect.

INTRODUCTION

Topological Insulators (TIs) are the materials which have conducting state on surface and its bulk behave like insulator [1, 2]. The existence of magnetism in topological insulator has become promising field to facilitatethe exotic phenomena viz. quantized magneto electric coupling and the axion insulator state. $MnBi_2Te_4$ is the recently proposed candidateas magnetic topological insulator (MTI) for Quantum Anomalous Hall Effect (QAHE) to occur due to its strong Spin-orbit coupling. $MnBi_2Te_4$forms an interlayer Anti-ferromagnetism (AFM) state, in which ferromagnetic (FM) Mn layers of neighbouring blocks are coupled anti-parallel to each other, converting the materialin a three-dimensional (3D) Anti-ferromagnetic TI. The reason of Magnetism is due to 3d metal which inserted into 3D topological insulator layers [3]. In case of MTIs, a magnetic layer or element is inserted among the running TI unit cells of bulk 3D topological insulators such as 3d metal doped Bi_2Se_3, Bi_2Te_3 and Sb_2Te_3 [4-6]. The insertion of magnetic layer along running 3D bulk topological insulators shifts the Dirac position and thus alters the quantum transport properties of theparent system [7-10]. One of the most fascinating properties of the MTIs is the appearance of Quantum Anomalous Hall (QAH) effect [7-9]. QAH happens due to the finite Hall voltage created due to magnetic polarization and spin-orbit coupling, while the external magnetic field is absent. QAH is found to be in integer multiple of e^2/h which is called Landau Level [9]. $MnBi_2Te_4$ can be formulated as Bi_2Te_3 + MnTe in which the MnTe, the magnetically ordered layer being inserted in the periodic structure at van der Waals gaps in $Bi_2Se_3$3D bulk topological insulator and later [14]. $MnBi_2Te_4$ is the first 3D antiferromagnetic topological insulator [11-13, 15]. Interestingly, there are only some reports on $MnBi_2Te_4$, in particular the single crystals [15].

EXPERIMENTAL

High-quality $MnBi_2Te_4$ single crystal has been grown by self-flux method through the conventional solid-state reaction route. High purity powders of Mn, Te and Bi were taken as starting material, weighed in stoichiometric ratio ground properly in glove box which is filled with argon (Ar) gas (or inert atmosphere) to avoid oxidation. Ground powder of $MnBi_2Te_4$was then palletized in rectangular form using hydraulic press then sealed into a quartz tube under the vacuum pressure 10^{-5}mBar. The vacuum sealed sample then kept into electric furnace with the rate of 2°C/min. up to 1000°C, kept there for 12 h and then slowly cooled down to 600°C at a rate of 1°C/h, again sample has been hold there for 12 h. Further, the furnace was allowed to cool naturally (20°C/Hour) to room temperature. Finally silvercolored shiny crystals were obtained (shown in Figure. 1(b)) which is mechanically

3rd International Conference on Condensed Matter and Applied Physics (ICC-2019)
AIP Conf. Proc. 2220, 110029-1–110029-4; https://doi.org/10.1063/5.0002194
Published by AIP Publishing. 978-0-7354-1976-6/$30.00

cleaved for further characterizations. The heat treatment diagram of as grown single crystal of $MnBi_2Te_4$ is shown in Fig.1(a).XRD pattern were performed on a Rigaku Made Mini Flex-II X-ray diffractometer while the magneto resistance measurements were carried out on a Physical Property Measurement System (PPMS-10Tesla) using a close cycle refrigerator.

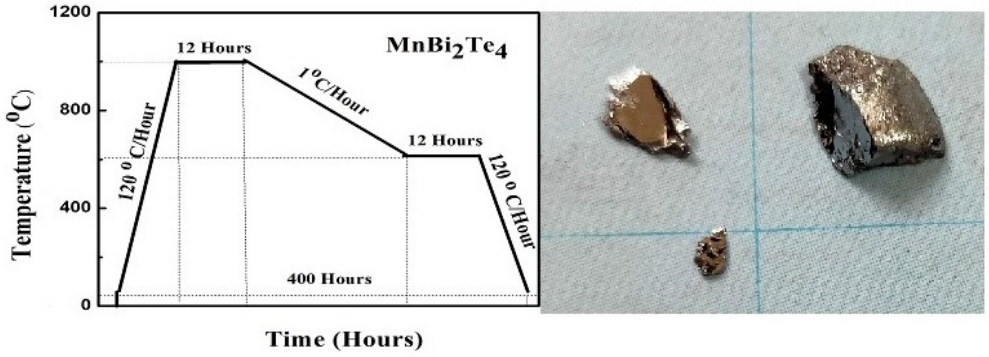

FIGURE 1.(a) Schematic heat treatment of $MnBi_2Te_4$ single crystal growth (b) As grown single crystal of same.

RESULTS AND DISCUSSION

Figure 2(a) depicts the X-ray diffraction pattern on flake of as grown $MnBi_2Te_4$ single crystal, which determines the crystallographic structure of the compound. The sharp XRD peaks of (0, 0, 4n) indicate the sample has been grown along the [00l] plane which confirms the highly crystalline nature of the studied sample.

The single phase fullprof Rietveld analysis is carried out on the observed pattern of crushed piece of $MnBi_2Te_4$ crystal shown in Figure 2(b). The PXRD pattern is similar to that as observed in some recent reports for $MnBi_2Te_4$ self flux grown crystal. The main phase $MnBi_2Te_4$ is found to be crystallized in rhombohedral structure having Space group R-3m. The lattice parameters are a=b=4.3882(1)Å and c=42.7125(1)Å. Some extra peaks of other phases i.e., $MnBi_6Te_{10}$, $MnBi_4Te_7$, MnTe and Bi_2Te_3 are also observed with the main phase which we have reported elsewhere [16].

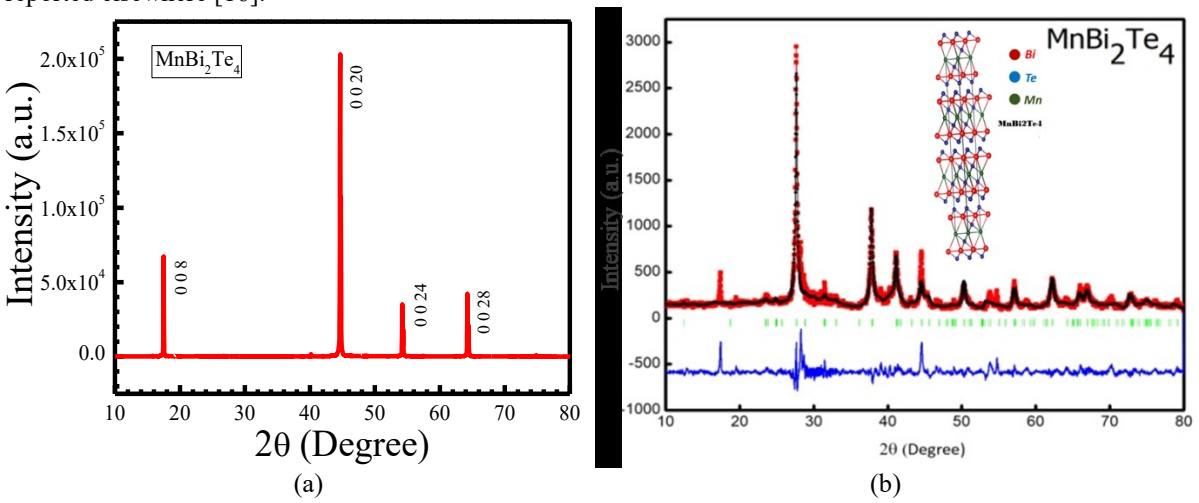

FIGURE 2. (a) X-ray diffraction pattern of flake of $MnBi_2Te_4$ single crystal (b) Rietveld refined PXRD pattern of $MnBi_2Te_4$ crystal and inset shows the unit cell of $MnBi_2Te_4$.

Inset of Figure 2(b) represents the unit cells for majority phase $MnBi_2Te_4$ drawn by VESTA software. The simplified general formula for these homologous series of compounds is given in the form of $MnTe+nBi_2Te_3$, with n = 0, 1, 2, 3 as $MnBi_2Te_4$, $MnBi_4Te_7$ and $MnBi_6Te_{10}$. So, principally it depends upon the fact that after how many unit cells of Bi_2Te_3, a MnTe magnetic layer is inserted.

Figure 3 shows the magneto-resistance percentage (MR%)versus applied magnetic field (H) at different temperature (10K, 20K, 50K and 200K) in applied magnetic field of up to 6Tesla for $MnBi_2Te_4$ single crystal. The MR (%) is calculated using the formula MR = $[\rho(H) - \rho(0)]/\rho(0)*100$, where $\rho(H)$ is the resistivity in the presence of magnetic field and $\rho(0)$ is resistivity in zero magnetic field. We observed non-saturating nearly linear positive MR value reaching up to 1.4% at 10K, whereas it reduces to around 0.8% when the temperature is

increased to 200K which is enormously less compared to as obtained in case of Bi_2Te_3 single crystal [17], shows the strong effect of magnetic ordering of Mn in MnTe layer of $MnBi_2Te_4$ crystal.

Inset of Figure 3 depicts the zoomed part of magneto-resistance measurement of $MnBi_2Te_4$ crystal in magnetic field range of ±1Tesla at 10K temperature. From the figure, it can be concluded that MR% decreases with increase magnetic field up to 0.2 Tesla, shows the –ve MR% on further increase in magnetic field the MR% increases and shows +ve MR% just above 0.5 Tesla, which further followed by almost linear behavior up to 1 Tesla magnetic field. It is also clear from the figure 3, that the MR% versus magnetic field plot for $MnBi_2Te_4$ crystal at low temperature shows almost linear behavior up to low field range of 0.2Tesla and shows the increment in MR% above the 0.2Tesla, which may be lead toward the quantum transport property like QAH. For confirmation about the observation of Quantum Anomalous Hall effect, detailed experiments are underway in different protocols in magnetic range up to 0.5 Tesla in very small step interval of field for $MnBi_2Te_4$ crystal.

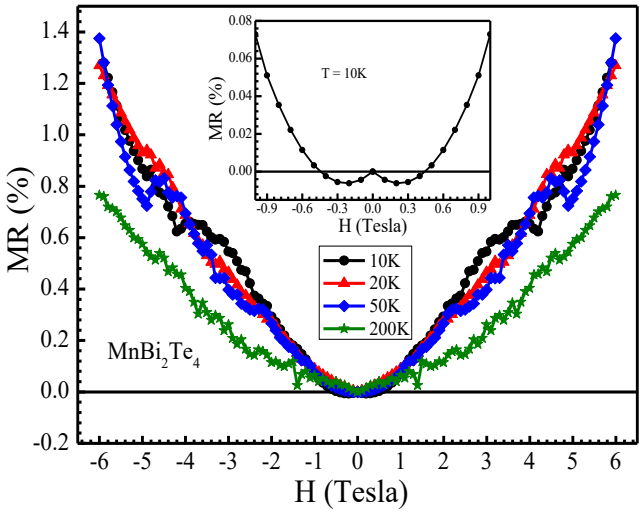

FIGURE 3. MR(%) as a function of magnetic field for the $MnBi_2Te_4$ single crystal at different temperatures.

CONCLUSION

In summary, in this the short communication we discuss the structural and magneto-resistance properties of the magnetic topological insulator $MnBi_2Te_4$. Detailed growth parameters have been discussed through XRD analysis.As long heat treatments are required to grow high quality single crystals so our crystal quality are defensible. Low temperature (10K) MR under magnetic field of up to 6 Tesla exhibited –ve MR below 0.5 Tesla and +ve for higher fields. The studied $MnBi_2Te_4$, MTI crystal could be a possible candidate for Quantum Anomalous Hall (QAH) effect.

ACKNOWLEDGMENTS

We thanks for CSIR-NPL & JNU for all experimental observation of data. Also we are thankful of DST for Fellowship facility. Currently we are working on it for better result and discovering new MTI.

REFERENCES

1. C. L. Kane and E. J. Mele, Phys. Rev. Lett. **95**, 146802-1-146802-4 (2005).
2. F. D. M. Haldane, Phys. Rev. Lett. **61**, 2015-2018 (1988).
3. L. Fu, C. L. Kane and E. J. Mele, Phys. Rev. Lett. **98**, 106803-1-106803-4 (2007).
4. Y. L. Chen, et al. Science, **325**, 178-181 (2009).
5. R. Sultana, P. Neha, R. Goyal, S. Patnaik and V. P. S. Awana, J. Magn. Mag. Mater. **428**, 213-218 (2017).
6. R. Sultana, G. Gurjar, S. Patnaik and V. P. S. Awana, Mat. Res. Exp. **5**, 046107 (2018).
7. C. X. Liu, S. C. Zhang and X. L. Qi, Annual Review of Condensed Matter **7**, 301-321 (2016).
8. C.-Z. Chang, J. Zhang, X. Feng, J. Shen, Z. Zhang, M. Guo, L. Minghua, O. Kang and W. P. Yunbo, Science **340**, 6129 (2013).
9. M. Z. Hasan and C. L. Kane, Rev. Mod. Phys. **82**, 3045-3067 (2010).
10. C. Z. Chang, W. W. Zhao, D. Y.Kim, H. J. Zhang, B. A.Assaf, D. Heiman, S. C.Zhang, C. X. Liu, M. H. W. Chan, and J. S. Moodera, Nature Materials, **14**, 473-477 (2015).

11. D. S. Lee, T. H. Kim, C. H. Park, C.Y. Chung, Y. S. Lin, W. S. Seo, H. H. Park, Cryst. Engg. Commun. **15**, 5532 (2013).
12. R. Visdal, H. Bentmann, T. Peixoto, A. Zeugner, S. Moser, C. Min, S. Schatz, K. Kissner, A. Unzelmann, C. Fornari et al., arxiv.1903.11826 (2019).
13. Y. Gong, J. Guo, J. Li, K. Zhu, M. Liao, X. Liu, Q. Zhang, L. Gu, L. Tang, X. Feng, et al.., arxiv.1809.07926 (2018).
14. J. Cui, M. Shi, H. Wang, F. Yu, T. Wu, X. Luo, J. Ying, X. Chen, Phys. Rev. B. **99**, 155125-1-155125-6 (2019).
15. J. Li, Y. Li, S. Du, Z. Wang, B. – L. Gu, S. – C. Zhang, K. He, W. Duan, Y. Xu, Science Advances , **5**, no. 6, DOI:10.1126/sxciadv.aaw5685
16. P. Rani, A. Saxena, R. Sultana, V. Nagpal, S. Patnaik, and V. P. S. Awana, arXiv:1906.09038 (2019).
17. R. Sultana, P. K. Maheshwari, B. Tiwari and V. P. S. Awana, Mat. Res. Exp. **5**, 016102 (2018).